Molecular Cell, Vol. 6, 1219–1232, November, 2000, Copyright ©2000 by Cell Press

# The Structure of Ribosome-Channel Complexes Engaged in Protein Translocation

**Jean-François Ménétret,*# Andrea Neuhof,†# David Gene Morgan,*†# Kathrin Plath,† Michael Radermacher,‡ Tom A. Rapoport,† and Christopher W. Akey*§**
*Department of Physiology and Biophysics
Boston University School of Medicine
Boston, Massachusetts 02118
†Howard Hughes Medical Institute and
Department of Cell Biology
Harvard Medical School
Boston, Massachusetts 02115
‡Max Planck Institut fur Biophysik
D-60528 Frankfurt
Germany

## Summary

**Cotranslational translocation of proteins requires ribosome binding to the Sec61p channel at the endoplasmic reticulum (ER) membrane. We have used electron cryomicroscopy to determine the structures of ribosome-channel complexes in the absence or presence of translocating polypeptide chains. Surprisingly, the structures are similar and contain 3–4 connections between the ribosome and channel that leave a lateral opening into the cytosol. Therefore, the ribosome-channel junction may allow the direct transfer of polypeptides into the channel and provide a path for the egress of some nascent chains into the cytosol. Moreover, complexes solubilized from mammalian ER membranes contain an additional membrane protein that has a large, lumenal protrusion and is intercalated into the wall of the Sec61p channel. Thus, the native channel contains a component that is not essential for translocation.**

## Introduction

Many secretory and membrane proteins are cotranslationally transported across or integrated into the endoplasmic reticulum (ER) membrane. Secretory proteins pass through the membrane completely, while membrane proteins cross it only part way and leave segments in the cytoplasm (reviewed in Hedge and Lingappa, 1997; Matlack et al., 1998). Both types of proteins are synthesized on membrane bound ribosomes and are transported through a protein-conducting channel in the ER membrane. How the translating ribosome binds to the channel is unknown.

A channel in the ER membrane was detected by conductance and fluorescence quenching experiments (Simon and Blobel, 1991; Crowley et al., 1994). The major component of the channel is the heterotrimeric Sec61p complex, which consists of an $\alpha$ subunit with ten transmembrane (TM) domains as well as smaller $\beta$ and $\gamma$ subunits, each with a single TM domain (reviewed in Matlack et al., 1998). The Sec61p complex is conserved among all eukaryotes and has a bacterial homolog, the SecYEG complex. Initial evidence that the Sec61p complex forms a channel came from crosslinking experiments that demonstrated its proximity to translocating polypeptide chains (Mothes et al., 1994). Subsequently, electron microscopy showed that the purified eukaryotic and prokaryotic complexes form similar ring-like structures both in detergent solution and in membranes (Hanein et al., 1996; Beckmann et al., 1997; Meyer et al., 1999). The size of these rings suggests that they are formed from multiple copies of the Sec61p or SecYEG complex.

Although reconstitution experiments demonstrated that the Sec61p complex is sufficient to form a membrane channel (Görlich and Rapoport, 1993), other components may be associated with the complex. Candidates include the *tr*anslocon-*a*ssociated *p*rotein (TRAP) complex and the *o*ligosaccharyl *t*ransferase (OST), both of which are tightly associated with native ribosome-channel complexes (Görlich et al., 1992). In the mammalian ER membrane, TRAP is abundant and consists of four subunits (Hartmann et al., 1993). However, its function is not known. The OST is a ubiquitous multisubunit complex whose primary role may be the glycosylation of nascent proteins (Silberstein and Gilmore, 1996).

The junction between the ribosome and the channel must play a critical role in the cotranslational transport of proteins across the ER membrane. According to the prevalent view, a continuous seal around the junction would guide the nascent chain from the ribosomal tunnel into the membrane channel. The existence of a tight seal between the ribosome and the channel is suggested by fluorescence quenching experiments (Crowley et al., 1994; Hamman et al., 1997). On the other hand, a three-dimensional (3D) analysis of soluble complexes between nontranslating yeast ribosomes and the purified yeast Sec61p complex indicated only one connection between the ribosome and the Sec61p complex, with a significant gap between them (Beckmann et al., 1997). However, the reconstitution of ribosome-Sec61p complexes in detergent and, in particular, the absence of a nascent chain make it difficult to assess the physiological significance of this observation.

The interaction between the ribosome and the channel is known to be dependent on the nascent polypeptide chain. Nontranslating ribosomes or ribosomes with short nascent chains bind weakly to the Sec61p complex and can be removed by high salt concentrations (Jungnickel and Rapoport, 1995). Ribosomes carrying long, translocating chains bind in a salt-resistant manner. Also, the ribosome-channel junction does not protect short nascent chains against proteolysis but does shield longer ones. The transition to a strong interaction occurs at a critical chain length (approximately 70 residues for preprolactin) and involves signal sequence recognition by the Sec61p complex and opening of the

§To whom correspondence should be addressed (e-mail: akey@med-biophm.bu.edu).
#These authors contributed equally to this paper.

channel toward the ER lumen (Jungnickel and Rapoport, 1995; Crowley et al., 1994). It is not clear whether the nascent chain causes a conformational change that increases the strength of the ribosome-channel interaction or if the chain merely provides an additional, stabilizing link.

While a continuous seal around the ribosome-channel junction would permit polypeptides, such as secretory proteins, to pass from the ribosome tunnel through the channel and into the ER lumen, it would present a problem in certain cases. For example, the transport of nascent membrane proteins must stop when a TM domain arrives within the channel to allow the following polypeptide segment to form a cytosolic domain. In this case the continuous connection between the ribosome and the channel would have to be broken to allow this segment to emerge into the cytosol.

To better understand the behavior of the ribosome-channel junction, we have determined the 3D structures of ribosome-channel complexes, both in the absence and presence of translocating nascent chains.

## Results

### Ribosomes Associated with Purified Sec61p Complexes

In a previous study, electron cryomicroscopy was used to determine the 3D structure of detergent-solubilized yeast Sec61p complex bound to yeast ribosomes lacking nascent chains (Beckmann et al., 1997). We repeated the structural analysis with complexes formed by binding ribosomes to the Sec61p complex in membranes, which created a more natural interaction. Isolated yeast ribosomes (Figure 1A, lane 1) were mixed with proteoliposomes containing the purified yeast Sec61p complex (lane 2), and unbound ribosomes were removed by floating the vesicles in a sucrose gradient. Ribosomes were found in the floated fraction only if the vesicles contained the Sec61p complex (lane 8 versus lane 5). The floated vesicles were then solubilized in digitonin, and the ribosomes were sedimented along with bound Sec61p complex (lane 9). In the absence of added ribosomes, no Sec61p complex was found in the pellet (not shown).

After resuspending the pellet, the ribosome-channel complexes were rapidly frozen and analyzed by electron cryomicroscopy. We used a yeast ribosome map (Morgan et al., 2000) as a first reference to determine the 3D structure of yeast ribosome-channel complexes. As a starting point, a threshold level was chosen for each structure so that the ribosome volume calculated from the density above the threshold would be consistent with its calculated volume (100% level).

Overall, the yeast ribosome-channel complex at approximately 25 Å resolution is similar to that reported by Beckmann et al. (1997) (Figure 2A shows a frontal view, and Figure 2B shows a view from the ER lumen; see Table 1 for statistics). The channel has an outer diameter of approximately 91 Å, and the nascent-chain exit site on the large ribosomal subunit is aligned with the pore (Figure 2C; the tunnel exit site is encircled by the gold channel outline). At this threshold, there is no visible connection between the ribosome and the Sec61p channel; hence, a sizable gap (approximately 20 Å) is present between them (Figure 2A). We conclude that the structural features of ribosome-channel complexes are essentially the same prior to solubilization, whether the ribosomes are directly bound to channels in detergent or bound to channels in membranes.

Next, we determined the structure of ribosome-channel complexes in which the ribosome carries a translocating nascent chain. We used rabbit reticulocyte ribosomes carrying the first 86 amino acids of preprolactin (86mer) as previous results have demonstrated that the 86mer induces a salt-resistant interaction of the ribosome with the channel and is fully inserted into the Sec61p channel (Jungnickel and Rapoport, 1995).

We first tested whether complexes of translating ribosomes and the Sec61p channel could be isolated. The 86mer was synthesized in a reticulocyte lysate in the presence of $^{35}$S-methionine. Proteoliposomes were added that contained purified canine Sec61p complex and the SRP receptor. The latter is required for membrane targeting of ribosome–nascent chain complexes. After translation, the vesicles were floated in a sucrose gradient at low (100 mM) or high (500 mM) salt concentration. In both cases, significant amounts of the 86mer were found in the floated fractions (Figure 1B, lanes 3–6) and remained bound to ribosomes as peptidyl tRNA, as demonstrated by precipitation with cetyltrimethylammonium bromide (CTABr; Figure 1B, lanes 4 versus 3 and 6 versus 5). Very little 86mer was found in floated vesicles that lacked the Sec61p complex and the SRP receptor (Figure 1C). When floated complexes containing the 86mer were solubilized in digitonin at high salt concentration and subjected to sedimentation, a portion of the 86mer was recovered in the pellet fraction (Figure 1B, lanes 7–10), and most of the material remained CTABr-precipitable (lanes 8 versus 7 and 10 versus 9). The complex of ribosome, 86mer, and Sec61p was very stable, even when it was generated with native membranes instead of proteoliposomes (Figure 1D). Most of the 86mer remained CTABr-precipitable for at least 5 hr (lanes 14 versus 13), and these results indicated that the nascent chain stayed associated with the ribosome as peptidyl tRNA. In addition, the nascent chain remained protease resistant, and this was indicative of its location inside the ribosome-channel complex (lanes 15 versus 13). Together, these data demonstrate that ribosome-channel complexes can be produced with a defined translocating nascent chain. Samples for electron cryomicroscopy were prepared similarly, except that the 86mer was synthesized in the absence of $^{35}$S-methionine.

To prepare control samples of the nontranslating ribosome-Sec61p complex, we added proteoliposomes to a nonprogrammed reticulocyte lysate. We followed this with flotation at low salt concentration and solubilization. Immunoblotting with an antibody to the ribosomal protein S26 showed that ribosomes were present in the final pellet fraction (Figure 1E, lane 2). No ribosomes were seen in the pellet if the flotation was performed at high salt concentration (lane 3), indicating that nontranslating ribosomes were effectively removed. It should be noted that solubilization of the complexes of nontranslating ribosomes and channels was carried out at high salt concentration. Upon solubilization in detergent, the interaction becomes salt resistant (Görlich et al.,

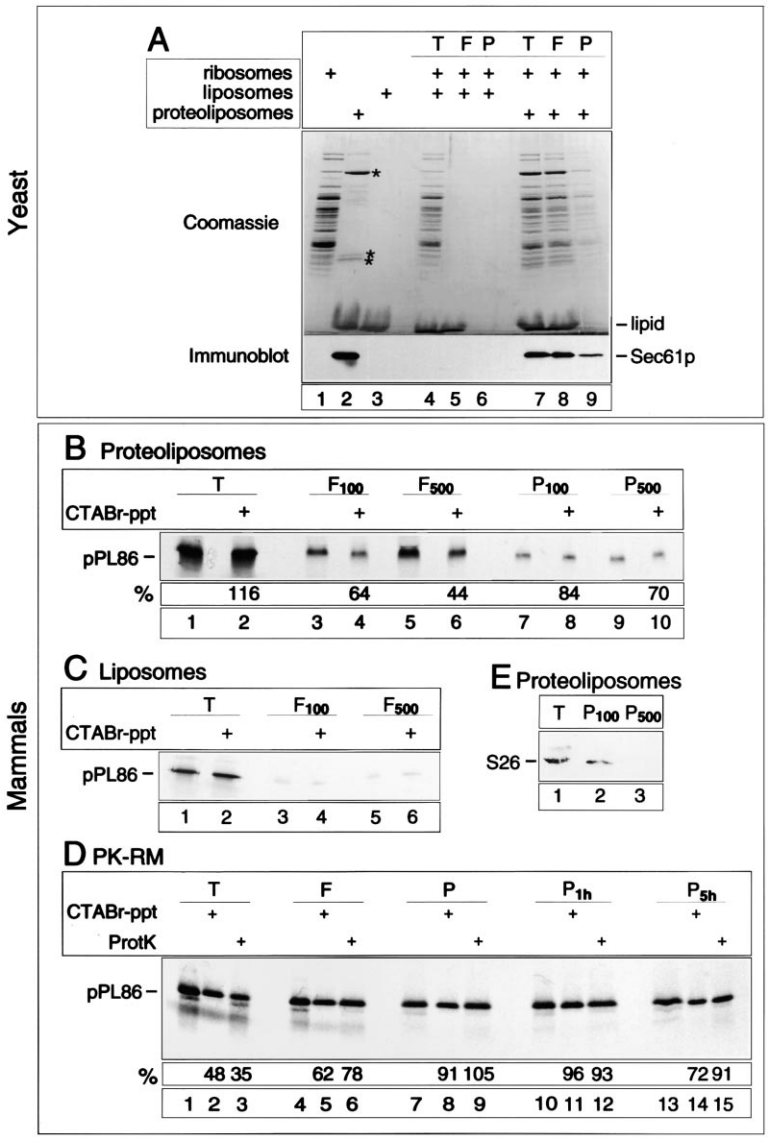


Figure 1. Isolation of Ribosome-Channel Complexes

(A) Yeast ribosomes were mixed with proteoliposomes containing purified yeast Sec61p complex (Sec61p) or with liposomes lacking protein. The membranes were floated in a sucrose gradient and solubilized in digitonin, and the ribosomes were sedimented. Equivalent aliquots of the individual components, of the original mixtures (T, for total), and of the floated (F) and pellet (P) fractions were subjected to SDS-PAGE and analyzed by staining with Coomassie blue or by immunoblotting with antibodies to Sec61p. The asterisks indicate the positions of the three subunits of the Sec61p complex.

(B) Radiolabeled 86mer of preprolactin (pPL86) was synthesized in a reticulocyte lysate in the presence of proteoliposomes containing canine Sec61p complex and SRP receptor. The membranes were floated in a sucrose gradient at either 100 or 500 mM salt and solubilized in digitonin at the appropriate salt concentration, and the ribosomes were sedimented. Equivalent aliquots of the original sample after translation (T), after flotation ($F_{100}$ and $F_{500}$) or after pelleting of the ribosomes ($P_{100}$ and $P_{500}$) were analyzed by SDS-PAGE followed by autoradiography. Each of the samples was also analyzed after precipitation with CTABr (CTABr-ppt). The percentage of CTABr-precipitable material is given below the lanes.

(C) As in (B), except that liposomes without protein were used.

(D) As in (B), except that ribosome-stripped native membranes (PK-RM) were used and flotation and solubilization were performed at 500 mM salt. All samples were analyzed by both CTABr precipitation and proteolysis with proteinase K (ProtK). The final pellet fraction was also incubated on ice for either 1 or 5 hr to test the stability of the ribosome-channel complex. Four times more material was loaded in F and P samples than in T samples.

(E) As in (B), except that a nonprogrammed translation mix was used and the ribosomes in the original sample (T; 10% loaded) and in the final pellet fraction (P) were detected by immunoblotting with an antibody to the ribosomal protein S26.

1992), in a manner similar to that observed with translating ribosomes on intact membranes.

A map of the rabbit ribosome (Morgan et al., 2000) was then used to determine the 3D structures of mammalian ribosome-channel complexes both without and with the preprolactin 86mer (Figures 2D–2F and 2G–2I; see Table 1). The structures were similar to those from yeast, except that the channel had a diameter of ~100 Å (compare Figures 2A and 2B with 2D and 2E). Surprisingly, there was little difference in the structures with and without a nascent polypeptide chain (compare Figures 2D and 2E with 2G and 2H). At the 100% threshold level, there was again no visible connection between the ribosomal large subunit and the Sec61p channel and a sizable gap (approximately 20 Å) was present between them (Figures 2D and 2G). When the threshold was lowered to enclose approximately 150% of the calculated ribosome volume, several connections were observed and the gap became narrower (Figures 2F and 2I). One of the connections appears to be in a position similar to that observed for the yeast complex (Beckmann et al., 1997).

### Ribosome-Sec61p Complexes Derived from Native Membranes

To test whether the structure of the ribosome-channel complex is altered in the presence of other ER components, we repeated the analysis with complexes produced from intact ER membranes. Ribosomes with and without the preprolactin 86mer were bound to canine microsomes stripped of ribosomes by a previous treatment with puromycin and high salt (PK-RM). Ribosome-channel complexes were prepared for electron microscopy, and their 3D structures were determined.

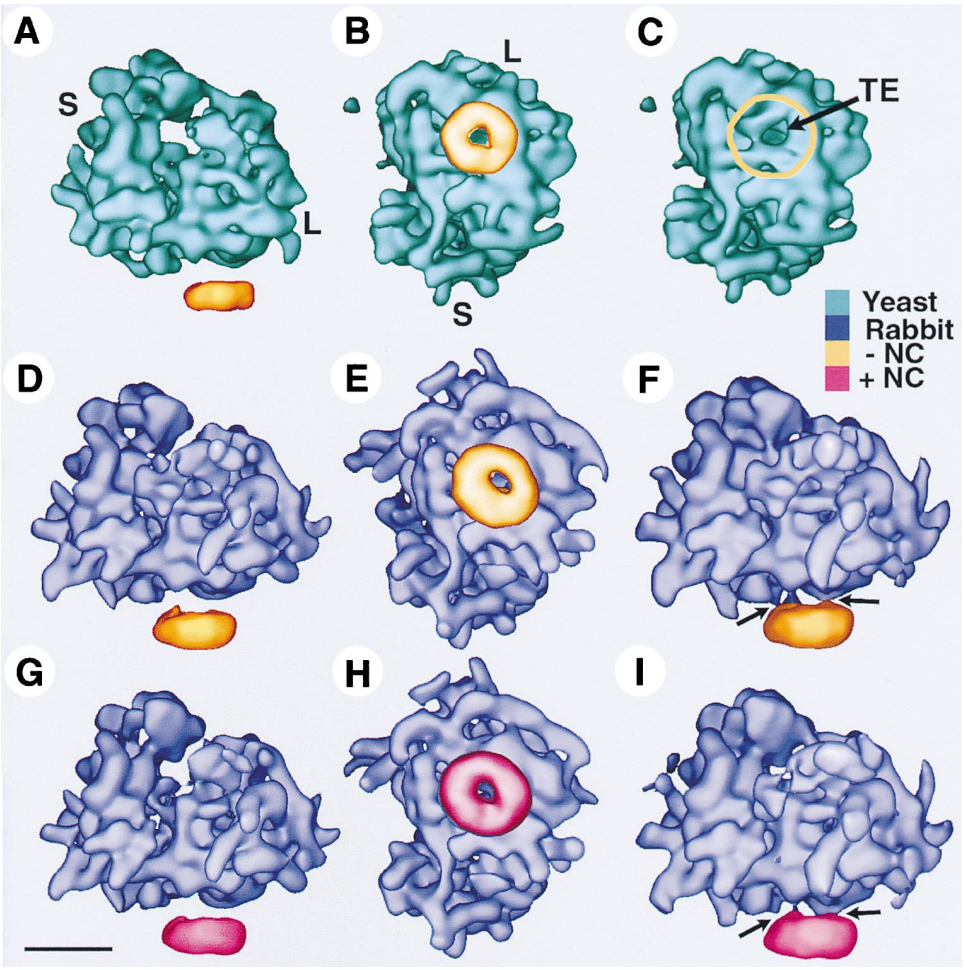


Figure 2. Ribosomes Associated with Purified Sec61p Complexes

(A) The complex of yeast ribosome (green) and yeast channel (gold) lacking a nascent chain is viewed along the plane of the ER membrane (frontal view). The threshold level was chosen to encompass 100% of the ribosomal volume. The small (S) and large (L) ribosomal subunits are indicated.

(B) The yeast complex is viewed from the ER lumen (bottom view). This view is generated by a 90° rotation about the horizontal axis, followed by a 90° rotation about the vertical axis in the plane.

(C) A similar view as in (B), with the circumference of the yeast channel outlined in gold to reveal the nascent chain tunnel exit (TE).

(D) The complex of rabbit ribosome (purple) and canine channel (gold), lacking a nascent chain, is shown in frontal view.

(E) The mammalian complex lacking a nascent chain shown in bottom view.

(F) The mammalian complex, lacking a nascent chain, is shown in frontal view with a threshold that encompasses approximately 150% of the expected ribosomal volume.

(G) The complex of rabbit ribosome (purple) and canine channel (red), with the 86mer of preprolactin present, is shown in frontal view.

(H) The mammalian complex with a nascent chain shown in bottom view.

(I) The mammalian complex with a nascent chain is shown in frontal view with a threshold that encompasses approximately 150% of the expected ribosomal volume.

Connections (c) between the channel and large subunit are indicated by arrows. Scale bar = 100 Å. The color code of the ribosomes and of the channels plus and minus nascent chain (NC) is shown as a vertical bar on the lower right.

The resulting structures demonstrate features that are similar to those seen previously (Figures 3A–3F). At a lower threshold (approximately 150%), multiple connections were observed between the ribosome and the channel (Figures 3C and 3F) at approximately the same positions (Figures 2F and 2I and Beckmann et al., 1997). However, the channels were noticeably larger and possessed an additional domain emerging from the lumenal side (to be discussed later). Although this feature was less pronounced when the 86mer was present, overall there were only small differences between the structures containing or lacking a translocating chain (Figures 3D–F versus 3A–C).

We wished to exclude the possibility that our results were biased by the choice of the preprolactin nascent chain or by the de novo assembly of ribosome-channel complexes in vitro. We therefore determined the 3D structure of native ribosome-channel complexes assembled in vivo in which the ribosomes carry a mixed population of endogenous nascent chains. Rough canine microsomes were washed with high salt to remove all ribosomes that do not carry translocating nascent

Table 1. Summary of Ribosome-ER Channel 3D Data Sets

| Ribosomes | Channels | Membranes | Nascent Chains | Particles | Resolution[a] (Å) |
|---|---|---|---|---|---|
| Solubilized | | | | | |
| Yeast | yeast | reconstituted vesicles | none | 9214 | 25 |
| Rabbit | canine | reconstituted vesicles | none | 9942 | 25 |
| Rabbit | canine | reconstituted vesicles | 86mer | 7902 | 25 |
| Rabbit | canine | native PK-RM | none | 6914 | 27 |
| Rabbit | canine | native PK-RM | 86mer | 6488 | 29 |
| Canine | canine | native K-RM | mixed | 6863 | 27 |
| Canine | canine | washed K-RM | mixed | 6847 | 29 |
| Canine | canine | reconstituted PK-RM | none | 4725 | 29 |
| Nonsolubilized | | | | | |
| Yeast | yeast | reconstituted vesicles | none | 4000 | 30 |
| Canine | canine | native (K-RM) | mixed | 200 | nd |

[a] Resolution was determined with the $FSC_{0.5}$ criterion. For each data set, pairs of 3D volumes were calculated with increasing numbers of particles up to the total number divided by two. The appropriate volumes were then compared, and their resolutions were plotted as a function of increasing particle number. This allowed us to estimate the resolution of the final complete 3D data sets by extrapolation.
The "nd" stands for "not determined."

chains. The membranes (K-RMs) were then solubilized in digitonin at high salt concentration, and the ribosome-Sec61p complexes were pelleted and analyzed by electron cryomicroscopy. Again, this 3D structure showed all the features seen previously (Figures 3G–I). As expected, the structure of the canine ribosome was similar to that of the rabbit ribosome, and the exit site of the nascent chain was aligned with the pore of the membrane channel (Figure 3I). Connections between the ribosome and the channel were only visible at lower threshold levels (compare the 100% level in Figure 3G with the 150% level in Figure 4A), and a gap was present.

In conclusion, the ribosome-channel junction does not change significantly, even when ribosomes carry a heterogeneous mixture of nascent chains at different stages of translocation. It should be noted that complexes containing a nascent chain did not show a significant density for peptidyl tRNA in the resulting structures, even though CTABr precipitation, protease-protection, and high-salt resistance all indicated the presence of a nascent chain. We believe that sample preparation and the nonphysiological mechanism used to terminate translation may have resulted in the peptidyl tRNA being distributed among approximately five possible binding sites on the ribosome (Agrawal et al., 2000). Hence, the tRNA density would be lost in the averaged structures.

### The Ribosome-Channel Junction

To analyze the ribosome-channel junction in more detail, we varied the threshold level, taking as an example complexes containing endogenous nascent chains derived from native membranes. When the threshold was lowered to include 200% of the ribosome volume, the background noise became significant (gray features in Figure 4B), and the pore was filled in (white contour in Figure 4C). Although this threshold level is clearly too low, a gap in the ribosome-channel junction is still visible as a pronounced lateral passage that leads from the ribosomal exit site to the cytosol (Figure 4C, dotted line). Therefore, we conclude that the gap is not dependent on the chosen threshold level and must be a genuine feature of the ribosome-channel junction.

Next, a statistical analysis was used to identify regions whose density was similar to that outside the ribosome, at a confidence level greater than 99% (blue contour in Figure 4D). These results illustrate that the gap between the ribosome and the channel is as empty as the protein-conducting tunnel in the ribosome. A similar analysis performed with all other structures confirmed that the gap is a general feature of the ribosome-channel junction.

Interaction sites between the ribosome and the channel were identified by lowering the threshold for all determined structures, to the point where individual connections could be seen. Bottom views of the ribosomes were then superimposed, and connections to the channel were marked (Figure 4E). The connections are shown as gray regions within the native channel, and the numbers indicate how many structures contributed to each. Three connections were located on one side of the tunnel exit in nine out of ten maps and are thus very likely real features. A fourth connection was present in only four maps. Together, they appear to form a horseshoe-like collar that provides a major lateral opening toward the cytosol (see arrow in Figure 4E). This opening is oriented approximately in the direction of the interface between the small and large ribosomal subunits. In Figure 4F the connections were overlayed onto a map of the native channel complex, which is contoured at a higher threshold level to indicate dense features that may correspond to ribosomal RNA. Interestingly, each of the connections to the channel was located over a high-density feature (Figure 4F). Together with a recent report demonstrating that the large subunit rRNA is sufficient to mediate interactions with the membrane channel (Prinz et al., 2000), these results suggest that several distinct rRNA regions may be involved.

To exclude the possibility that solubilization in detergent artificially generated a gap, we visualized ribosomes bound to intact membranes. Yeast ribosomes were incubated with proteoliposomes containing purified yeast Sec61p complex, and the vesicles were puri-

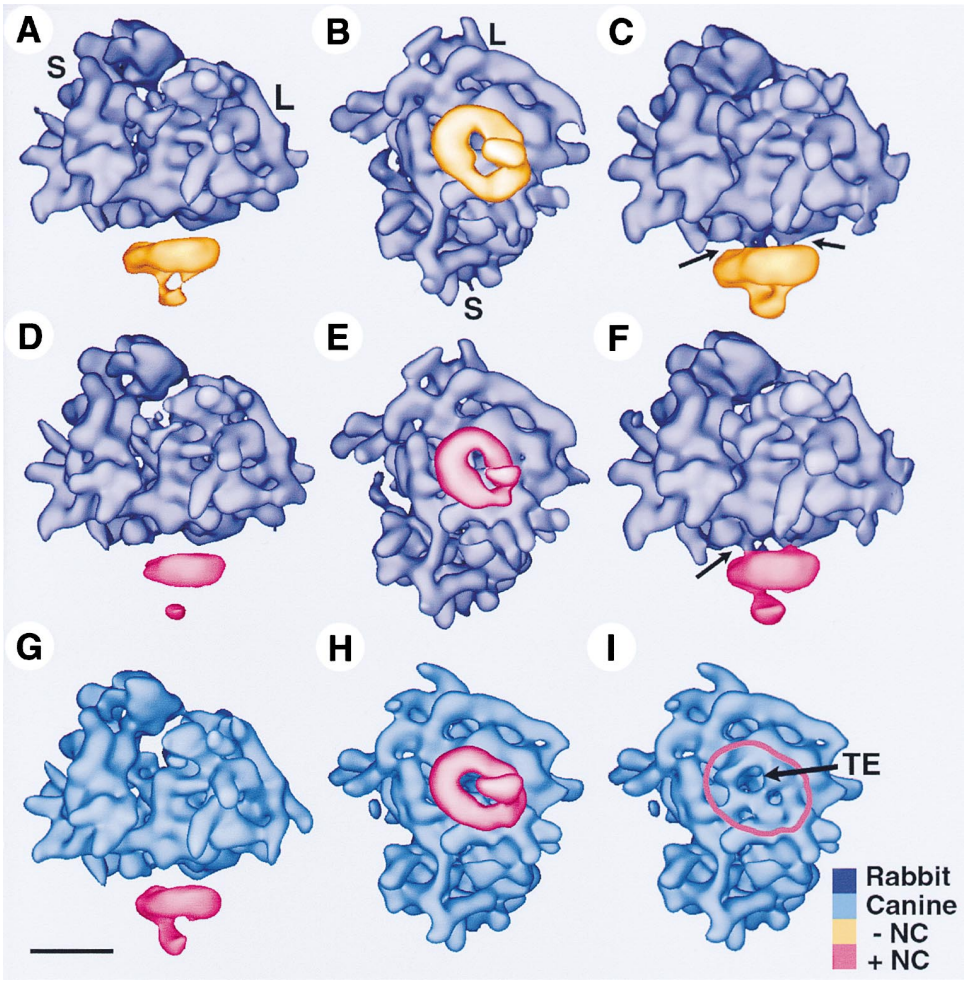


Figure 3. Ribosomes Associated with the Sec61p Complex Derived from Native Membranes

(A) The complex of nontranslating rabbit ribosomes (purple) and canine channels (gold), which was derived from ribosome-stripped membranes (PK-RM), is viewed along the plane of the ER membrane (frontal view). The threshold level was chosen to encompass 100% of the ribosomal volume. The small (S) and large (L) ribosomal subunits are indicated.

(B) The mammalian complex, derived from PK-RM, without a nascent chain is viewed from the ER lumen (bottom view). The threshold is at 100% ribosome volume.

(C) As in (A), with a threshold that encompasses approximately 150% of the expected ribosomal volume. Connections (c) between the channel and large subunit are indicated by arrows.

(D) The complex of rabbit ribosome (purple) and canine channel derived from PK-RM (red), with the 86mer of preprolactin present, is shown in frontal view.

(E) The mammalian complex, derived from PK-RM, with a nascent chain present is shown in bottom view. The threshold is at 100% ribosome volume.

(F) As in (D), with a threshold that encompasses approximately 150% of the expected ribosomal volume.

(G) The complex of canine ribosomes (blue) and canine channels (red), derived from native high salt–washed ER membranes (K-RM), with endogenous nascent chains present, is shown in a frontal view.

(H) The mammalian complex with endogenous nascent chains is shown in bottom view.

(I) A similar view as in (H), with the circumference of the canine channel outlined in red to reveal the nascent-chain tunnel exit. The smaller hole is only a dimple. Scale bar = 100 Å. The color code of the ribosomes and of the channels plus and minus nascent chain (NC) is shown as a vertical bar on the lower right.

fied by flotation. We collected images in which the ribosomes had the correct orientation relative to the plane of the membrane (Figure 5A and see Experimental Procedures). A 3D structure was calculated at approximately 30 Å resolution, and a projection along the vesicle edge demonstrates that there is a pronounced gap between the ribosome and the membrane (Figure 5A, left). A surface map, contoured at a threshold where the membrane is visible, shows that the gap is similar to that observed in solubilized complexes (Figures 5C versus 5E). This was verified by measuring the distance between recognizable features on the large ribosomal subunit and the middle of the membrane or channel (arrows in Figures 5C and 5E). Thus, the ribosome-channel junction does not change during solubilization. Although the channel is difficult to see because its density is similar to that of the membrane, a dense feature is observed at the expected position when the threshold level is raised (Figure 5D).

A similar analysis was performed with native mem-

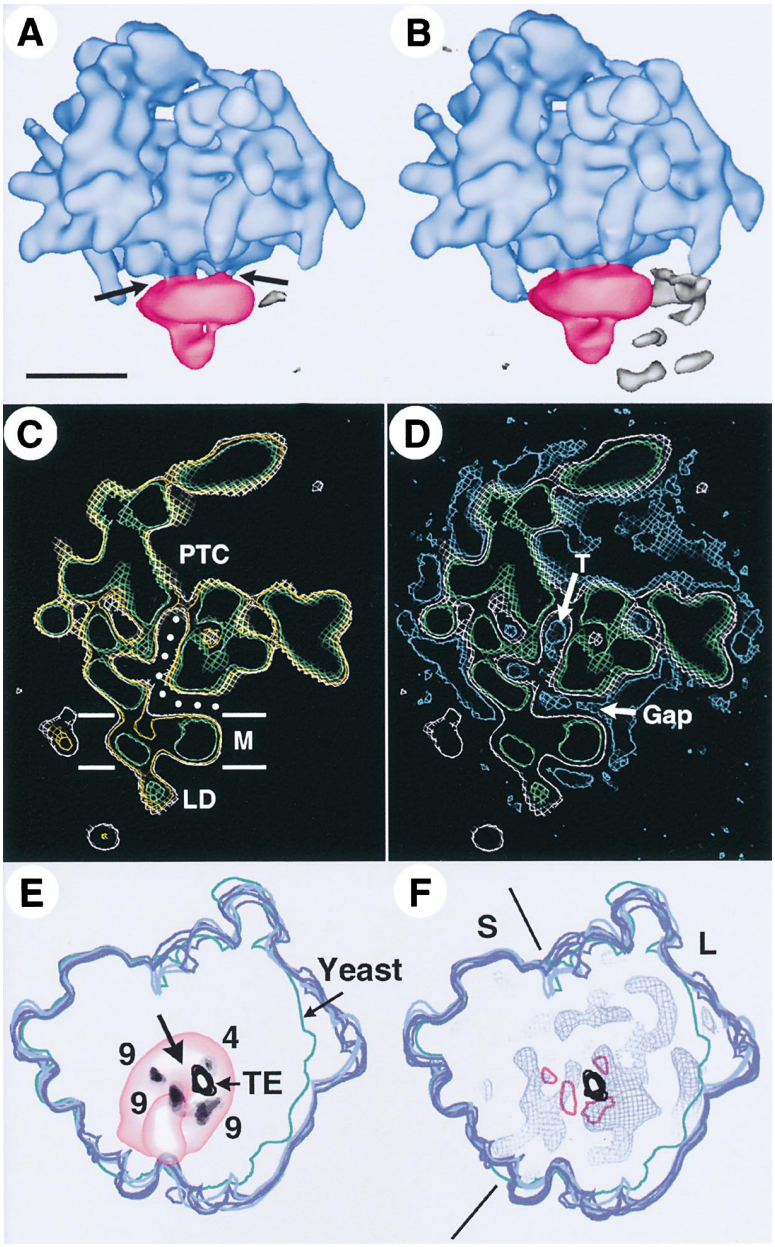


Figure 4. A Gap between the Ribosome and the Channel

(A) 3D structure of canine ribosome-channel complexes derived from native membranes. A mixed population of nascent chains is present. Shown is a frontal view at a threshold level corresponding to 150% of the ribosome volume. Arrows point to connections. Grey features indicate background noise. Scale bar = 100 Å.

(B) Similar view as in (A), except that the threshold was chosen to give a ribosomal volume of approximately 200%.

(C) A thin section is shown from the map, with the channel oriented at the bottom and the approximate position of the membrane (M) indicated. The map is contoured at three thresholds, corresponding to 100% (green), 150% (yellow), and approximately 200% (white). The gap and nascent chain exit tunnel (white dots) form a continuous path from the peptidyltransferase center (PTC) to the cytosol with a diameter of approximately 20 Å, even at a 200% threshold. Maps were displayed in "O" (Jones et al., 1991).

(D) A view similar to that in (C), with two thresholds for the ribosome-channel complex, 100% (green) and approximately 200% (white). Superimposed on this view is a statistical map (in blue), which defines regions that are lacking positive electron density (>99% confidence interval) and may correspond to solvent. The tunnel is labeled "T."

(E) The bottom views of ribosomes from ten structures, including the first 6 listed in Table 1 and four other unpublished maps, were superimposed, and connections to the channel were identified. These connections are shown as gray regions within the outline of a semitransparent native channel (the numbers indicate how many structures contributed to a connection). The tunnel exit (TE) is indicated, and a possible lateral opening for the nascent chain is marked with an arrow.

(F) A view similar to that in (E), with the connections overlayed in red onto high-density features (blue mesh) that surround the tunnel exit. The lines indicate the boundaries between the small (S) and large (L) ribosomal subunits.

brane bound ribosomes in salt-washed canine microsomes. Because of technical problems, we were able to analyze only approximately 200 particles to generate a low-resolution 3D structure. A projection of this structure (Figure 5B) also demonstrated that the spacing of the ribosome-membrane junction was similar to that observed in the yeast ribosome Sec61p vesicles. Therefore, we conclude that a gap is an intrinsic feature of the native ribosome-channel junction.

### Structure of the Translocation Channel

While the ribosome-channel junction is similar for structures derived from purified Sec61p complexes or from native membranes, the channels themselves differ significantly. Native channels contain a prominent lumenal domain (compare Figures 2 and 3) that is precisely oriented with respect to the ribosome and points toward the tunnel exit (Figure 4E). We estimate that the lumenal protrusion has a mass of about 100–150 kDa by comparison with the channel itself. In Figures 6A–6D, the channels from native membranes (K-RM) are compared with those formed by the purified Sec61p complex and are shown in isolation without the ribosome, either from the lumen of the ER (Figures 6A and 6B) or along the membrane plane (Figures 6C and 6D). The channels are presented at three different threshold levels (left to right), corresponding to a range that likely includes the true channel volume. When compared with purified Sec61p complexes (approximately 100 Å diameter), channels from native membranes are elliptical and larger (approximately 125 Å in the longest dimension). The increased channel size is consistent with previous results using freeze fracture electron microscopy (Hanein et al., 1996).

The channel formed by purified Sec61p complexes

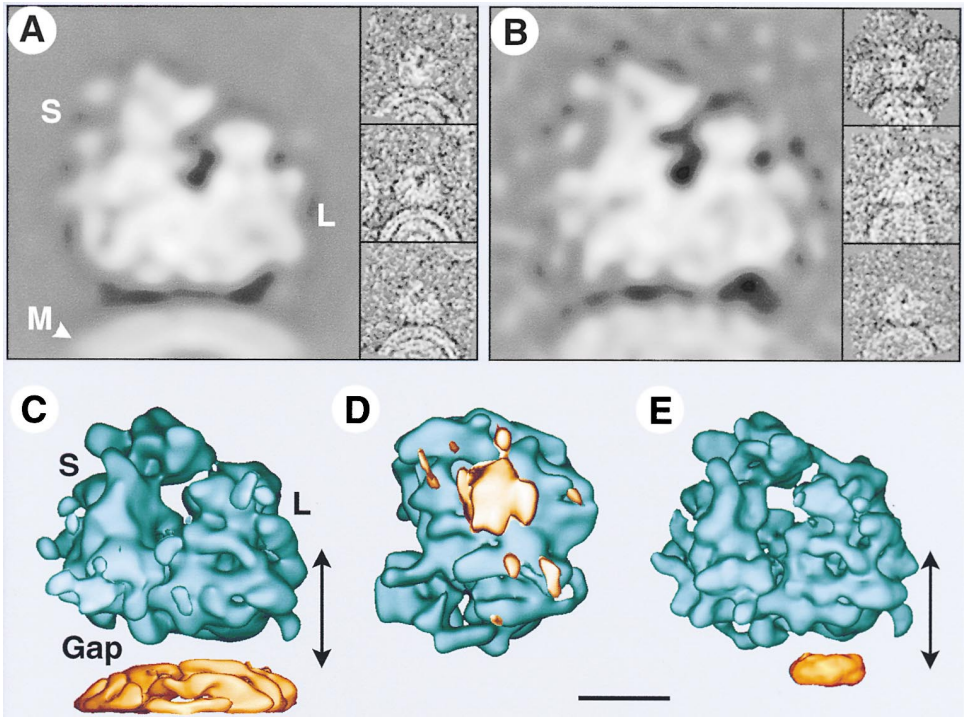


Figure 5. Interaction of Ribosomes with Membranes

(A) Three images of yeast ribosomes associated with channels in vesicles are shown on the right (protein and lipid are white). A projection map of the final 3D reconstruction is shown on the left. The small (S) and large (L) ribosomal subunits are labeled, and the membrane is indicated (M).

(B) Three images of canine ribosomes associated with channel complexes in native membranes (K-RM) are shown on the right. A projection map of the final 3D reconstruction is shown on the left.

(C) A 3D surface for the yeast ribosome-vesicle map is shown in the frontal view. A gap is seen between the ribosome (green) and the membrane (gold). The double arrow gives the distance between a recognizable feature on the ribosome to the center of the membrane.

(D) A bottom view of the yeast vesicle 3D map is shown at a higher threshold to reveal significant channel density over the nascent-chain exit tunnel.

(E) For comparison, a frontal view of the solubilized yeast ribosome-channel structure is shown. Note that the length of the double arrow is similar to that in (C). Scale bar = 100 Å.

has a cup shape with a large vestibule located toward the ribosome (approximately 50 Å diameter) that tapers to an approximately 20 Å pore on the lumenal side (Figure 6E). The complex from which the channel was taken did not have a nascent chain; however, similar channel structures were obtained with the chain present (see Figures 2D–2I). The channel derived from native membranes looks similar to the purified channel when sectioned along the short axis (Figure 6F, middle panel). In a section cut approximately 45° away, the pore is both larger and maintains a constant diameter (Figure 6F, right panel). The central pore of the native channel extends from a point opposite the ribosomal tunnel exit to the site where the lumenal protrusion emerges (the pore size is approximately 20 × 50 Å at the 110% threshold level). When purified channels are overlayed with those derived from native membranes, their similarity in the region over the ribosome tunnel exit is apparent (Figures 6G and 6H, center panels), while major differences are seen where the lumenal domain emerges from the channel (Figure 6H, central panel). Importantly, large-scale differences were not detected between channels that differ by the presence of a nascent chain. Specifically, the pore size remained the same, unlike what was seen in fluorescence quenching experiments using native membranes (Hamman et al., 1997, 1998).

### Native Channels Contain an Additional Membrane Protein

We first tested whether soluble, lumenal proteins contribute to the structural difference between native and purified channels. Native membranes (K-RM) were extracted with digitonin at low salt concentrations to remove most lumenal proteins (Figure 7A, $S_o$tot) and then used to generate ribosome-channel complexes. The determined structure was identical to that obtained with nonextracted membranes and showed the lumenal domain (compare Figures 3G and 7B). This result was confirmed by the use of proteoliposomes reconstituted from a crude detergent extract of ribosome-stripped microsomes. The vesicles were incubated with nontranslating ribosomes and subjected to the usual procedure to generate ribosome-channel complexes. The structure of these complexes (Figure 7C) indicates that they are similar to those obtained from native membranes, although they appear to have a lower channel occupancy as evidenced from the disconnected lumenal domain and smaller channel size.

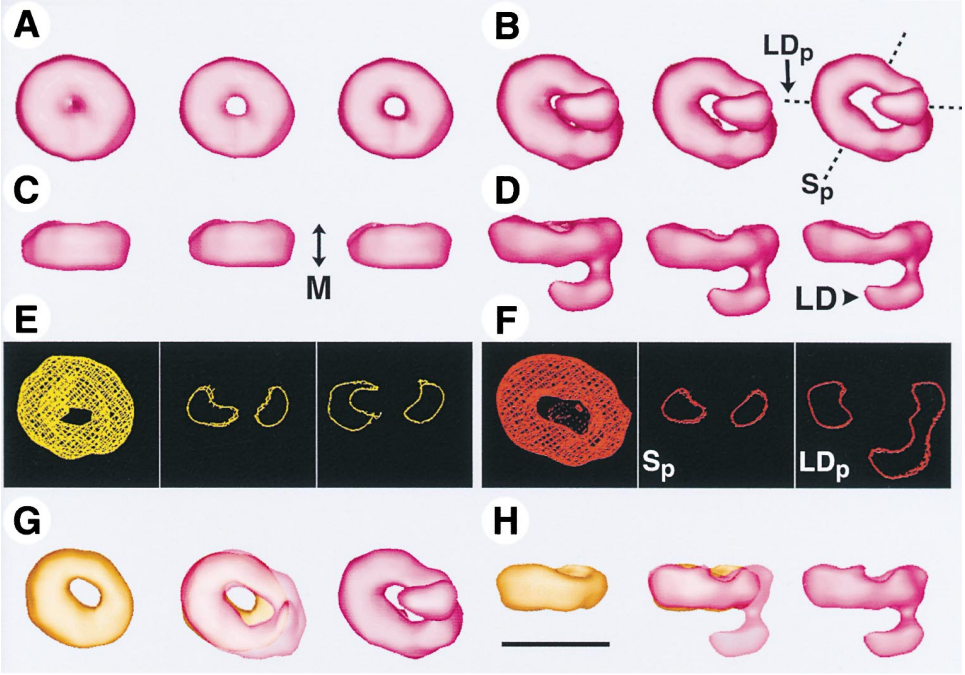


Figure 6. Structure of the Translocation Channel

(A) The purified canine Sec61p channel in the presence of the 86mer of preprolactin is viewed from the ER lumen at thresholds equivalent to 120%, 110%, and 100% of the associated ribosome volume.

(B) The canine channel derived from native membranes in the presence of a mixed population of nascent chains is viewed from the ER lumen at a threshold series as in (A).

(C) As in (A), but viewed from the side along the membrane plane.

(D) As in (B), but viewed from the side along the membrane plane. The lumenal domain (LD) is indicated.

(E) The purified canine Sec61p channel in the absence of a nascent chain is shown in gold as a wiremesh surface viewed from the ribosome (left panel). The center and right panels show slices through the channel. These slices correspond to a view along the shortest axis and a view offset by approximately 45°, respectively.

(F) The canine channel in the presence of a mixed population of nascent chains is shown in orientations similar to those in (E).

(G) An overlap view (center panel) of the two maps from the left panels in (E) and (F) is shown. The native channel is semitransparent, and the lumenal domain has been removed. The original maps are shown on either side.

(H) An overlap view (center panel) of the two maps from the right-most panels in (E) and (F) are shown. The native channel is semitransparent. The original maps are shown on either side. Scale bar = 100 Å.

Next we determined which membrane proteins are present in the complexes used for structural analysis of native channels. The ribosome-channel pellet, which would normally be analyzed in the microscope, was resuspended and treated with puromycin and high salt to dissociate the ribosomes and release associated membrane proteins (Görlich et al., 1992). The ribosomal subunits were sedimented, and the supernatant was analyzed either directly by SDS-PAGE (Figure 7A, $S_p$tot) or after extraction with Triton X-114 to enrich for integral membrane proteins ($S_p$TX-114). As expected, this fraction contained the Sec61p complex. In addition, it contained the TRAP and OST complexes (indicated with symbols in the figure). Immunoblot analysis demonstrated that the majority of these proteins were released from the ribosomes by puromycin treatment (not shown). A number of other proteins, including signal peptidase and TRAM, that were involved in translocation were not present in the ribosome-channel complex. Therefore, we conclude that either the TRAP or OST complex is responsible for the differences between native and purified channels.

## Discussion

Two major conclusions can be deduced from our structural analysis. First, the junction between the ribosome and the channel is not continuous, and a lateral opening to the cytosol is always present. Second, channels derived from native membranes differ significantly from those formed by the purified Sec61p complex. They contain either the TRAP or OST complex, which contribute to the formation of a lumenal protrusion.

### A Gap between the Ribosome and the Channel

Beckmann et al. (1997) demonstrated the existence of a sizable gap between the ribosomal large subunit and the ER channel. This gap was believed to be due to the lack of a nascent chain. We now provide evidence that the ribosome-channel interaction does not become more extensive when a translocating nascent chain is present. We consider it unlikely that the gap between the ribosome and the membrane channel is an artifact for several reasons. First, it has now been seen in 15 3D structures by using different methods of complex

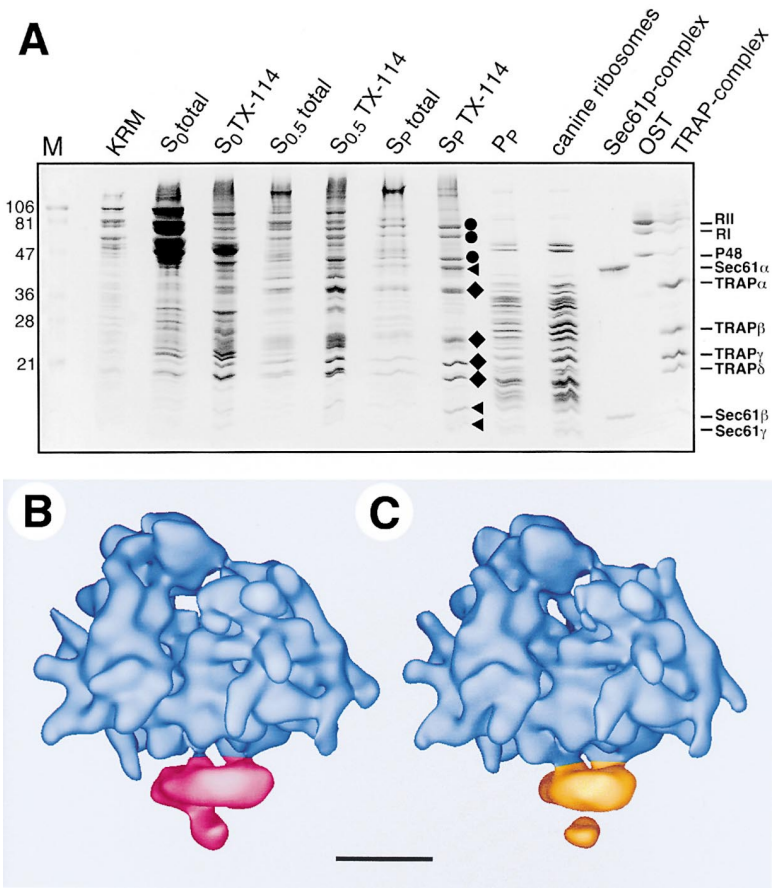


Figure 7. A Lumenal Protrusion in Native Channels Formed Either by TRAP or OST

(A) Pancreatic microsomes washed with high salt (K-RM) were extracted in digitonin without salt. This resulted in a supernatant (tot; 10 eq loaded) and a pellet fraction. The pellet was extracted first with a buffer containing digitonin and 0.5 M salt, which resulted in a supernatant ($S_{0.5}$tot, 10 eq) and a pellet containing ribosomes and associated membrane proteins. To release the membrane proteins, the pellet was treated with puromycin in digitonin at 1.2 M salt. After centrifugation, a supernatant ($S_P$tot, 50 eq) and a pellet ($P_P$, 5 pmol ribosomes loaded) were obtained. To enrich for membrane proteins, a portion of all supernatant fractions was extracted with Triton X-114, and the detergent phase was analyzed ($S_0$TX-114 (20 eq), $S_{0.5}$TX-114 (20 eq), $S_P$TX-114 (100 eq). All samples were subjected to SDS-PAGE and analyzed by staining with Coomassie blue. Lanes 9–12 show purified canine ribosomes, Sec61p, OST, and TRAP complexes. Dots, triangles, and diamonds indicate subunits of the OST, Sec61p, and TRAP complexes, respectively.

(B) Native membranes (K-RM) were extracted with digitonin at low salt concentrations to remove most lumenal proteins. The membranes were subjected to the usual procedure to generate ribosome-channel complexes, and their structure was determined.

(C) Ribosome-stripped microsomes (PK-RM) were solubilized in deoxyBigCHAP at high salt concentration, and the extract was treated with hydrophobic beads to remove the detergent. The resulting proteoliposomes were incubated with nontranslating ribosomes and solubilized, and a structure was determined.

formation, sources of material, and methods of analysis. Second, the presence of a gap is not dependent on the chosen threshold level. Even at unrealistically low thresholds, there is at least one lateral passage with a diameter of approximately 20 Å leading from the tunnel exit of the ribosome to the cytosol. Third, the gap is seen with ribosome-channel complexes in intact membranes.

Although the existence of a gap between the ribosome and the channel appears likely, there is still the possibility that it contains some material that is not visible at this resolution (25–27 Å). For example, flexible segments of ribosomal RNA or proteins or of the Sec61p complex may be present. In addition, we cannot exclude conformational changes caused by the nascent chain that are below the resolution limit. As the three or four connections between the ribosome and the channel were seen only at low thresholds, we suggest that they are small or flexible. However, by acting together they may stably tether the channel to the ribosome.

The existence of a gap between the ribosome and the channel does not contradict previous data that demonstrated that polypeptides passing into the lumen of the ER are protected against externally added proteases (Connolly et al., 1989); the gap is too narrow to allow access of a protease to the translocating polypeptide chain. The data are also consistent with electrophysiological experiments showing that a nascent chain prevents the passage of ions through the membrane (Simon and Blobel, 1991) if one assumes that the block occurs within the membrane channel. However, our results are more difficult to reconcile with fluorescence quenching data that show the existence of a seal for ions between the ribosome and the channel. For example, fluorescent probes in short preprolactin chains of 56 or 64 amino acids could not be quenched by iodide ions added to the cytosolic compartment (Crowley et al., 1994). Perhaps the diffusion of iodide ions is inhibited by charges on the ribosome and/or the channel surfaces lining the pathway or by flexible material. It should also be noted that the same short nascent chains can be cleaved by protease (Jungnickel and Rapoport, 1995). This finding supports the existence of a lateral opening between the ribosome and channel.

If the ribosome-membrane junction does not form a seal, then how is the permeability barrier maintained between the ER lumen and the cytosol? One possibility is that the nascent chain in the channel provides sufficient hindrance to the flow of small molecules and that the channel is disassembled when it is not in use. A more provocative idea would be that the active channel provides only a minimal hindrance to the flow of small molecules. A leaky ER membrane channel may not cause problems in maintaining gradients if pumps such as the $Ca^{2+}$ ATPase are active enough.

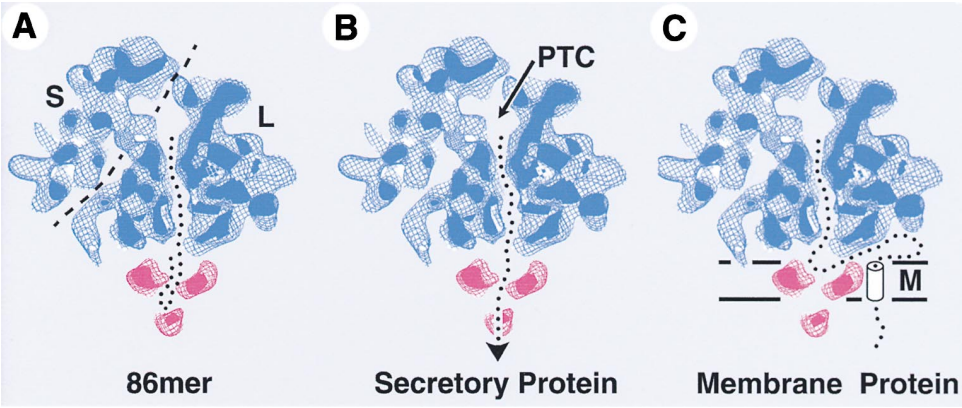


Figure 8. Possible Pathways for the Nascent Chains of Secretory and Membrane Proteins

(A) A thin section was generated from the 3D structure of the ribosome-channel complex derived from native canine membranes. Internal solid surfaces revealed by the front cutting plane are filled with blue. The channel is colored in red. The predicted position of the preprolactin 86mer that extends from the peptidyltransferase center (PTC) to the channel is indicated by a dotted line. The chain likely adopts a loop structure and is representative of early stages of translocation. The small (S) and large (L) ribosomal subunits are labeled, and the boundary between them is marked by a dashed line.

(B) The possible path for secretory nascent chains from the PTC to the ER lumen is indicated.

(C) The possible path of a nascent membrane protein is shown when a cytosolic domain is being synthesized following the integration of a TM segment into the membrane (M).

A gap between the ribosome exit site and the membrane channel raises the question of how the polypeptide chain is translocated. Early during translocation, when a nascent secretory protein contains approximately 60 residues, the signal sequence will have emerged from the ribosomal tunnel, but the chain would be too short to insert into the Sec61p channel as a loop. The flexible N termini of these chains may sometimes extend through the gap into the cytosol, and this would explain why they are accessible to proteolysis (Jungnickel and Rapoport, 1995). With nascent chains longer than approximately 70 residues the signal sequence would be inserted into the pore as a result of its affinity for a specific binding site in the channel wall (Plath et al., 1998; see Figure 8A). Insertion of the signal sequence as a loop would guide the following part of the polypeptide chain into the channel pore so that no part would be exposed to the cytosol. This would explain why such chains are protease resistant. As the chain is elongated during translation, polypeptide segments would pass from the ribosomal tunnel, cross the gap, and emerge through the pore in the Sec61p channel into the ER lumen (Figure 8B). The polypeptide chain would normally pass in the forward direction during translation as the gap may be narrow enough to prevent polypeptide segments from looping out into the cytosol.

The existence of a gap simplifies models of how cytosolic segments of membrane proteins may escape through the ribosome-channel junction. We propose that the ribosome-channel junction remains unchanged or undergoes only small conformational changes when a hydrophobic membrane anchor stops the transfer of the polypeptide chain through the channel. The membrane anchor may then exit the channel laterally and drag the nascent chain with it through the gap in the ribosome-channel junction. It would thus allow the following segment to emerge into the cytosol (Figure 8C). Even if the gap contained flexible material, it would not be expected to totally block the egress of the nascent chain. As the nascent chain is further elongated, it would emerge from the membrane bound ribosome close to the cytosolic end of the Sec61p channel, and its hydrophobicity could thus be continuously probed. If sufficiently hydrophobic, the segment would insert into the channel as a loop and reinitiate translocation of a lumenal domain.

A similar model would apply to translocational pausing during the synthesis of certain secretory proteins, such as apolipoprotein B (Hedge and Lingappa, 1996). In this case, a nonhydrophobic "pause-transfer" sequence would stop polypeptide movement through the channel and lead to the transient looping of a polypeptide segment into the cytosol. A lateral opening between the ribosome and the channel may also explain how nascent polypeptides can be transported backward from the ER lumen into the cytosol, despite the ribosome being bound to the channel (Ooi and Weiss, 1992). Finally, should ribosomes synthesizing cytosolic proteins bind to the channel, the existence of a passageway into the cytosol would allow them to continue translation.

### The Native Protein Translocation Channel

Our results reveal that native channels contain an integral membrane protein that is distinct from the Sec61p complex and that may correspond to either the TRAP or OST complex. However, a structural comparison of the native and purified channels suggests that the size difference may arise from only one of the two membrane complexes. Neither of these proteins is essential for protein translocation (Migliaccio et al., 1992; Görlich and Rapoport, 1993). Thus, our data indicate that nonessential membrane proteins are recruited to the native translocation channel.

Interestingly, the lumenal protrusion formed by the additional component is precisely oriented within the ribosome-channel complex even though it does not

make direct contact with the ribosome. Because the Sec61p channel itself is asymmetric (Hanein et al., 1996), the additional component may become associated at a specific site. The additional membrane protein also causes drastic changes in the channel. This component seems to be intercalated into the walls of the Sec61p channel and to increase the size of the membrane-embedded portion. In addition, it changes the shape and size of the pore. In the purified channel the central pore is cylindrical, with a diameter of about 20 Å on its lumenal side, whereas in the native channel the pore is elliptical, with a size of approximately 20 × 50 Å. The purified Sec61p channel has a cup-like cross section with a rather narrow constriction toward the lumen. This shape is similar to the funnel-like shape observed by Beckmann et al. (1997). The shape would be ideal to collect the nascent chain when it begins to emerge from the ribosome and could restrict its lateral movement. The small lumenal opening may also restrict the passage of other molecules through the membrane when the nascent chain is present. The channel derived from native membranes has a uniform cross section along its major axis that may be more suitable for ongoing translocation. During the initiation of translocation, perhaps one state of the channel is converted into the other by the recruitment of the membrane component that forms the lumenal protrusion.

If the additional component is OST, its function would be obvious; the tip of the lumenal protrusion may recognize glycosylation sites in the nascent chain and attach a carbohydrate chain. On the other hand, TRAP appears to be more abundant in the ribosome-channel complex, and its size is more consistent with the changes in the membrane domain and the size of the lumenal protrusion. There are a total of seven TM domains, and three of the four TRAP subunits have lumenal domains. In addition, TRAP$\alpha$ can be crosslinked to nascent chains in the ER lumen, whereas no crosslinks have been detected with OST (Mothes et al., 1994). The function of TRAP is currently unknown. However, it may enhance the translocation efficiency of some proteins, be involved in interactions with lumenal chaperones or modification enzymes, or regulate the opening of the pore.

## Experimental Procedures

### Preparation of Ribosomes and Membrane Vesicles

Yeast and rabbit reticulocyte ribosomes were purified as described (Morgan et al., 2000). The purification of canine SRP receptor and canine and yeast Sec61p complexes as well as their reconstitution into proteoliposomes were carried out as described (Görlich et al., 1993; Jungnickel and Rapoport, 1995; Hanein et al., 1996). Canine microsomes were stripped of ribosomes with puromycin and high salt (PK-RMs) (Neuhof et al., 1998). Salt-washed canine microsomes (K-RM) were prepared similarly, except that the puromycin treatment was omitted.

### Preparation of Ribosome Channel Complexes

Transcripts coding for preprolactin 86mer were produced by in vitro transcription with the Ribomax SP6 kit (Promega) (Jungnickel and Rapoport, 1995). The mRNA was translated in rabbit reticulocyte lysate in the presence of either PK-RMs or proteoliposomes containing purified SRP receptor and Sec61p complex for 20 min at 27°C. To generate complexes lacking a nascent chain, the mRNA was omitted. After translation, 1-acyl-2-(6-[7-nitro-2,1,3-benzoxadiazole-4-yl amino]-caproyl)-sn-glycero-3-phosphocholine (C6-NBD-PC) in ethanol was added to a final concentration of 1 mol% of total phospholipid to follow the fractionation of membranes under UV light. The translation mixture was adjusted to a final volume of 150 μl containing either 2 M sucrose (PK-RMs) or 1.5 M sucrose (proteoliposomes), both in 30 mM HEPES/KOH (pH 7.8) and 10 mM magnesium acetate buffer. For ribosomes with or without a nascent chain, the buffer also contained 500 mM or 100 mM potassium acetate, respectively. The samples were transferred to a 7 × 20 mm polycarbonate tube (Beckman), overlayed with 30 μl of the same buffer without sucrose, and spun for 1 hr at 100,000 rpm at 2°C in a Beckman TLA100 rotor. A UV transilluminator was used to visualize the floated membranes. They were diluted about 1:3 in buffer containing 30 mM HEPES/KOH (pH 7.8); 10 mM magnesium acetate; 1.5% digitonin (final concentration); and 100 mM potassium acetate for proteoliposomes with ribosomes lacking nascent chains or 500 mM potassium acetate for samples containing nascent chains and for all PK-RM samples. After incubation for 15 min at 4°C, the samples were centrifuged for 20 min at 100,000 rpm at 2°C in a TLA100 rotor. The pellet was resuspended in 30 mM HEPES/KOH (pH 7.8), 1.5% digitonin, 100 mM potassium acetate, and 10 mM magnesium acetate. Aliquots were analyzed by SDS-PAGE and immunoblotting against the $\alpha$ and $\beta$ subunits of the Sec61p complex. CTABr precipitation and treatment with proteinase K were done as described (Mothes et al., 1997). All samples were kept at 4°C and frozen for electron cryomicrosocopy within approximately 4 hr of preparation.

Preparation of yeast ribosomes with bound Sec61p was similar to that of the mammalian complexes lacking nascent chains except that purified ribosomes were used. Yeast ribosomes bound to reconstituted proteoliposomes containing the yeast Sec61p complex were isolated by flotation and directly analyzed by electron microscopy.

### Enrichment of Membrane Proteins Associated with Ribosomes

K-RM (180 equivalents [eq]) were extracted at 0.5 eq/μl with buffer A (50 mM HEPES [pH 7.8], 1.5% digitonin, 10 mM magnesium acetate, 2 mM dithiothreitol, 1:1000 protease inhibitors). The sample was centrifuged for 40 min at 70,000 rpm in a Beckman TLA100.3 rotor at 4°C in microfuge tubes. The pellet was resuspended at 0.5 eq/μl in buffer A containing 0.5 M potassium acetate. After the removal of aggregates in a microfuge, the samples were centrifuged for 40 min at 70,000 rpm in a TLA100.3 rotor. The pellet was resuspended at 0.5 eq/μl in buffer A containing 1.2 M potassium acetate. Puromycin (2 mM) and GTP (1 mM) were added, and the sample was incubated for 30 min on ice and 15 min at 37°C. It was subsequently spun for 40 min at 70,000 rpm in a TLA100.3 rotor. The pellet was resuspended at 3 eq/μl in 50 mM HEPES (pH 7.8), 250 mM sucrose, 150 mM potassium acetate, and 2 mM magnesium acetate. The absorbance at 260 nm was determined, and 5 pmol of ribosomes were loaded for SDS-PAGE. A sample containing 50 eq of the supernatants was used to analyze the protein composition. Proteins were precipitated with 20% PEG and the pellet was washed in methanol and subjected to SDS-PAGE. The supernatants (100 eq) were subjected to Triton X-114 extraction as described by Görlich et al. (1992).

### Electron Cryomicroscopy of Ribosome-Channel Complexes

Suspensions were loaded onto 300 mesh grids, with thin continuous carbon film supported by a holey carbon mesh, that had been previously glow-discharged in air. The specimens were blotted and plunged into liquid ethane (Dubochet et al., 1988) in a humid environment at 4°C (>85% relative humidity). A Gatan cryotransfer system and cryoholder (model 626-DH) were used to transfer grids into a Philips CM12 transmission electron microscope equipped with a cryoblade–type anticontaminator and specimen relocation system. All electron micrographs were recorded at 100 kV under minimal dose conditions with a $LaB_6$ filament, and a defocus range of −1 to −2 μm was used. Micrographs were recorded at 28,000× magnification on KODAK SO163 film and developed for 12 min in full-strength D19 developer (KODAK). In some cases, images were recorded with the specimen tilted at 30° by using a dynamic defocus spot scan package developed by Dr. I. Tews.

### Three-Dimensional Image Processing and Analyses

Micrographs were inspected by optical diffraction, and those displaying minimal astigmatism and drift were chosen for processing.

Entire negatives were digitized with a Zeiss SCAI scanner by using a 7 μm raster, binned to a pixel size of 14 μm (corresponding to 5 Å/pixel), and converted to SPIDER format (approximately 5000 × 6000 pixels). Image processing was done with the SPIDER software package (Frank et al., 1996). In most cases, particle picking was semiautomated. The image was first cross-correlated against a reference calculated by rotationally averaging the frontal view of the yeast ribosome. Image features with a cross-correlation peak higher than 0.5 were windowed (128 × 128 pixels) from the original micrographs, montaged, and interactively deselected to remove bad particles. In difficult cases, particles were picked interactively from large sections of the original micrograph in WEB. Each precentered, 2D dataset of ribosome-channel complexes was first aligned against the corresponding ribosome model truncated to approximately 50 Å resolution by using Radon alignment methods (Radermacher, 1994). Multiple alignment cycles were done as described previously (Morgan et al., 2000), and final 3D volumes were obtained by R-weighted back projection. We restricted the resolution of the final maps so that the CTF does not play a critical role in forming the gap (Morgan et al., 2000).

The threshold representing 100% of the ribosomal volume was chosen on the basis of calculated and experimentally measured partial specific volumes and the known mass of ribosomal protein and RNA. The 100% ribosomal volumes used in this work were $3.75 \times 10^6$ Å$^3$ (yeast) and $4 \times 10^6$ Å$^3$ (mammals).

A statistical 3D map was computed for each structure by randomly breaking the data set into subsets containing 500 particles and generating their R-weighted 3D maps. These maps were averaged to produce a 3D volume, and its statistical significance was determined (Trachtenberg and DeRosier, 1987).

### Processing of Ribosomes on Intact Membranes

Ribosomes bound to small vesicles (approximately 300–500 Å diameter) were generally seen in edge views. To select ribosomes bound to channels, we took advantage of the fact that they should freely rotate about an axis perpendicular to the membrane plane; nonspecifically bound ribosomes should adopt all possible angular orientations. An initial 2D alignment was used to place the membranes in a similar orientation. The soluble yeast ribosome-Sec61p complex was used as a reference after the rotation of this map so that 3D rotation around the axis normal to the membrane could be readily identified. After iterative cycles of alignment, images whose alignment angles differed significantly from those expected were eliminated, and the updated reference was obtained by R-weighted back projection.

All particles were evaluated with a second procedure to test for genuinely bound ribosomes. A model 3D volume was constructed with an idealized vesicle surface passing through the Sec61p channel within the 3D map of the yeast ribosome-channel complex. This model was then projected at the 3D alignment angles determined for each particle, which allowed a visual comparison of the predicted and actual positions of the membrane. When these two images agreed, the ribosome was considered to be associated with an underlying channel. Overall, there was good agreement in the particles selected with either criteria.

### Acknowledgments

We thank I. V. Akey for yeast ribosomes, J. Stahl for antibodies to S26, and K. Matlack for help with experiments, suggestions, and critical reading of the manuscript. J. F. M. was supported by NIH training grants, and D. G. M. was supported by the HHMI. Both the C. W. A. and T. A. R. laboratories are supported by NIH grants, and T. A. R. is a Howard Hughes Medical Institute investigator.

Received August 16, 1999; revised September 29, 2000.

### References

Agrawal, R.K., Spahn, C.M., Penczek, P., Grassucci, R.A., Nierhaus, K.H., and Frank, J. (2000). Visualization of tRNA movements on the *Escherichia coli* 70S ribosome during the elongation cycle. J. Cell Biol. *150*, 447–460.

Beckmann, R., Bubeck, D., Grassucci, R., Penczek, P., Verschoor, A., Blobel, G., and Frank, J. (1997). Alignment of conduits for the nascent polypeptide chain in the ribosome-Sec61 complex. Science *19*, 2123–2126.

Connolly, T., Collins, P., and Gilmore, R. (1989). Access of proteinase K to partially translocated nascent polypeptides in intact and detergent-solubilized membranes. J. Cell Biol. *108*, 299–307.

Crowley, K.S., Liao, S.R., Worrell, V.E., Reinhart, G.D., and Johnson, A.E. (1994). Secretory proteins move through the endoplasmic reticulum membrane via an aqueous, gated pore. Cell *78*, 461–471.

Dubochet, J., Adrian, M., Chang, J.-J., Homo, J.-C., Lepault, J., McDowall, A.W., and Schultz, P. (1988). Cryo-electron microscopy of vitrified specimens. Quarterly Review of Biophysics *21*, 129–228.

Frank, J., Radermacher, M., Penczek, P., Zhu, J., Li, Y., Ladjadj, M., and Leith, A. (1996). SPIDER and WEB: processing and visualization of images in 3D electron microscopy and related fields. J. Struct. Biol. *116*, 190–199.

Görlich, D., Prehn, S., Hartmann, E., Kalies, K.U., and Rapoport, T.A. (1992). A mammalian homolog of Sec61p and SecYp is associated with ribosomes and nascent polypeptides during translocation. Cell *71*, 489–503.

Görlich, D., and Rapoport, T.A. (1993). Protein translocation into proteoliposomes reconstituted from purified components of the endoplasmic reticulum membrane. Cell *75*, 615–630.

Hamman, B.D., Chen, J.C., Johnson, E.E., and Johnson, A.E. (1997). The aqueous pore through the translocon has a diameter of 40–60 Å during cotranslational protein translocation at the ER membrane. Cell *89*, 535–544.

Hamman, B.D., Hendershot, L.M., and Johnson, A.E. (1998). BiP maintains the permeability barrier of the ER membrane by sealing the lumenal end of the translocon pore before and early in translocation. Cell *92*, 747–758.

Hanein, D., Matlack, K.E.S., Jungnickel, B., Plath, K., Kalies, K.-U., Miller, K.R., Rapoport, T.A., and Akey, C.W. (1996). Oligomeric rings of the Sec61p complex induced by ligands required for protein translocation. Cell *87*, 721–732.

Hartmann, E., Görlich, D., Kostka, S., Otto, A., Kraft, R., Knespel, S., Burger, E., Rapoport, T.A., and Prehn, S. (1993). A tetrameric complex of membrane proteins in the endoplasmic reticulum. Eur. J. Biochem. *214*, 375–381.

Hedge, R.S., and Lingappa, V.R. (1996). Sequence-specific alteration of the ribosome-membrane junction exposes nascent secretory proteins to the cytosol. Cell *85*, 217–228.

Hedge, R.S., and Lingappa, V.R. (1997). Membrane protein biogenesis: regulated complexity at the endoplasmic reticulum. Cell *91*, 575–582.

Jones, T.A., Zou, J.-Y., and Cowan, S.W. (1991). Improved methods for building protein models in electron density maps and the location of errors in these models. Acta Crystallogr. A *47*, 110–119.

Jungnickel, B., and Rapoport, T.A. (1995). A posttargeting signal sequence recognition event in the endoplasmic reticulum membrane. Cell *82*, 261–270.

Matlack, K.E.S., Mothes, W., and Rapoport, T.A. (1998). Protein translocation: tunnel vision. Cell *92*, 381–390.

Meyer, T.H., Ménétret, J.F., Breitling, R., Miller, K.R., Akey, C.W., and Rapoport, T.A. (1999). The bacterial SecY/E translocation complex forms channel-like structures similar to those of the eukaryotic Sec61p complex. J. Mol. Biol. *285*, 1789–1800.

Migliaccio, G., Nicchitta, C.V., and Blobel, G. (1992). The signal sequence receptor, unlike the signal recognition particle receptor, is not essential for protein translocation. J. Cell Biol. *117*, 15–25.

Morgan, D.G., Ménétret, J.F., Rademacher, M., Neuhof, A., Akey, I.V., Rapoport, T.A., and Akey, C.W. (2000). A comparison of the yeast and the rabbit 80S ribosome reveals the topology of the nascent chain exit tunnel, inter-subunit bridges and mammalian rRNA expansion segments. J. Mol. Biol. *301*, 301–321.

Mothes, W., Prehn, S., and Rapoport, T.A. (1994). Systematic probing of the environment of a translocating secretory protein during translocation through the ER membrane. EMBO J. *13*, 3937–3982.

Mothes, W., Heinrich, S.U., Graf, R., Nilsson, I., von Heijne, G., Brunner, J., and Rapoport, T.A. (1997). Molecular mechanism of membrane protein integration into the endoplasmic reticulum. Cell *89*, 523–533.

Neuhof, A., Rolls, M.M., Jungnickel, B., Kalies, K.-U., and Rapoport, T.A. (1998). Binding of signal recognition particle gives ribosome/nascent chain complexes a competitive advantage in endoplasmic reticulum membrane interaction. Mol. Biol. Cell *9*, 103–115.

Ooi, C.E., and Weiss, J. (1992). Bidirectional movement of a nascent polypeptide across microsomal membranes reveals requirements for vectorial translocation of proteins. Cell *71*, 87–96.

Plath, K., Mothes, W., Wilkinson, B.M., Stirling, C.J., and Rapoport, T.A. (1998). Signal sequence recognition in posttranslational protein transport across the yeast ER membrane. Cell *94*, 795–807.

Prinz, A., Behrens, C., Rapoport, T.A., Hartmann, E., and Kalies, K.-U. (2000). Evolutionarily conserved binding of ribosomes to the translocation channel via the large ribosomal RNA. EMBO J. *19*, 1900–1906.

Radermacher, M. (1994). Three-dimensional reconstitution from Radon projections: orientational alignment via Radon transforms. Ultramicroscopy *53*, 121–136.

Silberstein, S., and Gilmore, R. (1996). Biochemistry, molecular biology, and genetics of the oligosaccharyl transferase. FASEB J. *10*, 849–858.

Simon, S.M., and Blobel, G. (1991). A protein-conducting channel in the endoplasmic reticulum. Cell *65*, 371–380.

Trachtenberg, S., and DeRosier, D.J. (1987). Three dimensional structure of the frozen-hydrated flagellar filament: the left handed filament of *Salmonella typhimurium*. J. Mol. Biol. *195*, 581–601.